

ANVIL: Anomaly-based Vulnerability Identification without Labelled Training Data

Weizhou Wang*, Eric Liu†, Xiangyu Guo‡ and David Lie§

University of Toronto

Canada

Email: {*weizhou.wang, †ec.liu, ‡xiangyu.guo}@mail.utoronto.ca, §david.lie@utoronto.ca

Abstract—Supervised learning-based software vulnerability detectors often fall short due to the inadequate availability of labelled training data. In contrast, Large Language Models (LLMs) such as GPT-4, are not trained on labelled data, but when prompted to detect vulnerabilities, LLM prediction accuracy is only marginally better than random guessing. In this paper, we explore a different approach by reframing vulnerability detection as one of anomaly detection. Since the vast majority of code does not contain vulnerabilities and LLMs are trained on massive amounts of such code, vulnerable code can be viewed as an anomaly from the LLM’s predicted code distribution, freeing the model from the need for labelled data to provide a learnable representation of vulnerable code. Leveraging this perspective, we demonstrate that LLMs trained for code generation exhibit a significant gap in prediction accuracy when prompted to reconstruct vulnerable versus non-vulnerable code.

Using this insight, we implement ANVIL, a detector that identifies software vulnerabilities at line-level granularity. Our experiments explore the discriminating power of different anomaly scoring methods, as well as the sensitivity of ANVIL to context size. We also study the effectiveness of ANVIL on various LLM families, and conduct leakage experiments on vulnerabilities that were discovered after the knowledge cutoff of our evaluated LLMs. On a collection of vulnerabilities from the Magma benchmark, ANVIL outperforms state-of-the-art line-level vulnerability detectors, LineVul and LineVD, which have been trained with labelled data, despite ANVIL having never been trained with labelled vulnerabilities. Specifically, our approach achieves $1.62\times$ to $2.18\times$ better Top-5 accuracies and $1.02\times$ to $1.29\times$ times better ROC scores on line-level vulnerability detection tasks.

I. INTRODUCTION

Probabilistic approaches to static vulnerability detection have garnered considerable research attention due to the promise of automatically detecting common bug patterns by training a model on historical data. Confidence in statistical modelling has only grown with the recent advances in large language models (LLMs). One of the significant advantages of LLMs is that they can be trained in a self-supervised fashion without labelled training data. This has enabled them to be trained on very large training sets. This approach has led to impressive and surprising results in code understanding and code generation [1], [2].

Unfortunately, the same cannot be said about their ability to detect vulnerabilities. As shown in a recent study [3], even with cutting edge LLMs like GPT-4, vulnerability prediction accuracy on real world code is little better than a coin-flip.

Current learning and LLM-based vulnerability detectors [4]–[11] suffer from the same lack of a large and well-labelled set of representative vulnerabilities. Attempts to compensate for the dearth of labelled data by selecting relevant code features (e.g. the granularity of the code context, commit history, control-flow, data-flow, etc.) and converting these features into a learnable representation (e.g. a vector, a graph, etc.) have only yielded modest improvements. Similarly, recent attempts to generate new vulnerable training corpora [12]–[14] have not improved real-world performance significantly, as synthetically generated vulnerabilities still cannot capture the huge variety of ways that vulnerabilities can manifest.

LLMs are effective because they can learn a general feature space from a large training set. This does not lend itself well to understanding vulnerable code patterns due to a fundamentally imbalanced corpora. Out of the huge amounts of unlabelled code that LLMs are trained on, only a miniscule portion will contain vulnerabilities. Instead of attempting to learn bug patterns from this sparse signal, we advocate for the inverse. Since bugs are inherently *anomalous*, we believe that LLMs should be leveraged as a model for correct code. If we accept that code LLMs are capable of generalizing the structure of bug-free code, then bug detection can be cast as an anomaly detection problem.

There have been previous attempts at modelling software defects and vulnerabilities as anomalous code. For example, studies of code “naturalness” [15], [16] have shown that source code contains many of the same characteristics as natural language and hence can be modelled by statistical methods. Subsequent work has then found a statistically significant difference between buggy and fixed code when measuring the entropy of predictions from a n -gram model trained on 35 million LOC, which enabled their approach to achieve bug detection that was competitive with static-analysis based tools.

However, modern transformer-based LLMs have considerably greater representational power than n -gram models, and are trained on data sets with 10’s-100’s of billions of LOC (a 4-5 order of magnitude increase!). We hypothesize that such models will be far more capable of exploiting the insight that vulnerabilities are just anomalous code. But, modern LLMs also introduce a number of new challenges when applying them to anomaly-based vulnerability detection. First, modern LLMs are so accurate at predicting code, that they often predict correct code almost perfectly. In such cases,

an entropy measure may underestimate the level of an anomaly between a perfect and an almost-perfect prediction, motivating an exploration of methods for measuring the anomaly level of predictions. Second, unlike the previous generation of n -gram models, LLMs can use a context of hundreds to thousands of tokens to make predictions, raising the question of the appropriate context size to use. Third, given the availability of a variety of industrially-trained open-source models of varying sizes and architectures, we find ourselves in a position to explore whether this approach truly generalizes to different model architectures, and how it performs as models scale to larger capacities and training sets. Finally, given that modern LLMs are trained on large training sets of code, there is a risk that a pre-trained LLM may have seen both the vulnerable and fixed version of some code – commonly referred to as “leakage”. We evaluate our approach on a leakage-free dataset we created that only contains vulnerabilities found after the training date of the LLMs we use to demonstrate that our results generalize to unseen vulnerabilities.

To summarize, we make the following contributions:

- We propose an anomaly-based vulnerability detection method, ANVIL, that leverages the learned knowledge of pre-trained LLMs. We demonstrate that masked code reconstruction accuracy is an effective way to differentiate between vulnerable and non-vulnerable code.
- We evaluate different parameters for our masked span reconstruction technique, namely the model size and prompt context. From our experiments, larger models and compound statement contexts enable more accurate vulnerability detection.
- Our anomaly-based tool performs favourably with LineVul [8] and LineVD [9], two detectors that were trained to predict line-level vulnerabilities.

We make all code for our tool ANVIL available at <https://anonymous.4open.science/r/anvil>. All data and scripts used for running our evaluation are also made public for reproducibility.

II. METHODOLOGY

A. Overview

Similar to previous research in code naturalness, we consider a span of code anomalous (i.e. unnatural) if a model considers it out-of-distribution. Specifically, the feedback we utilize is the LLM reconstruction accuracy on a code generation task, when masking each span of code for inference. LLMs are trained to predict the most probable token given a chain of previous tokens, hence a low reconstruction accuracy compared to the ground truth indicates that the ground truth has deviated from the learned representation of the model. Figure 1 describes the workflow of our technique, ANVIL. For each line of code under analysis, we withhold the original line as the ground truth and instruct the LLM to reconstruct it based on the surrounding context. The LLM generated code is then compared with the ground truth to compute an *anomaly score*, which quantifies the divergence between them.

B. FIM & Context Selection

Code LLMs are trained to perform specific generative tasks, such as code-completion, where the model is trained to predict the next n tokens given a code prefix, or fill-in-the-middle (FIM, also known as infilling) [17], where the model is trained to generate tokens that fall between a given prefix and suffix.

We focus on the utility of FIM as the mode of code generation for detecting anomalies. Although code completion is a more prevalent task, research by Bavarian et al. [17] highlights that FIM tasks generally result in lower reconstruction loss due to additional constraints provided by the suffix. This structure allows FIM to capture downstream control and data flows, which are crucial for generating correct code for a masked line.

However, adapting the FIM task for anomaly detection introduces several challenges due to constraints such as GPU memory and LLM token limits, which make it impractical to use entire source files as context. To address this, we empirically evaluate two methods for finding a context size: (1) a fixed size approach and (2) a semantics-aware approach. For (1), we investigate the effect of fixing the context to a specific number of source-code lines, equally split between the prefix and suffix. For instance, a 500-line context means using 250 lines preceding and succeeding the line under analysis.

Alternatively, (2) adaptively selects the maximum compound statement (MCS) surrounding the line under analysis. In C/C++, a compound statement refers to a sequence of statements enclosed by curly braces (“{” and “}”). Given a line of source code, we define the MCS as the largest compound statement that encapsulates the line. For each line, ANVIL statically extracts the MCS to use as the context. Often, the MCS equates to the function body containing the line; however, if the MCS is too large, exceeding token limits or GPU memory capacity, we resort to the next largest compound statement that meets these constraints. We note that this technique is agnostic to the hardware used, but empirically, we found that a context limit of 500 lines reached near-maximum peak usage of our GPU memory. Hence, our adaptive MCS selection only considers compound statement that are 500 lines or fewer.

```

PNG_FUNCTION(voidpf /* PRIVATE */,
png_zalloc,(voidpf png_ptr, uint items, uint size),PNG_ALLOCATED)
{
    png_alloc_size_t num_bytes = size;
    if (png_ptr == NULL)
        return NULL;
    if (items >= (png_alloc_size_t)0/size)
        <FILL ME>
        return NULL;
    num_bytes = items;
    return png_malloc_warn(png_voidcast(png_structrp, png_ptr), num_bytes);
}

```

Fig. 2. An example from *libpng* showing the largest and second-largest compound statement for a line of interest

If no suitable compound statement is identified, we default to providing a prefix and suffix of 150 lines each. This choice is based on empirical data from our experiments, where a context window of 300 lines, among all fixed context sizes, struck the best balance between GPU memory utilization

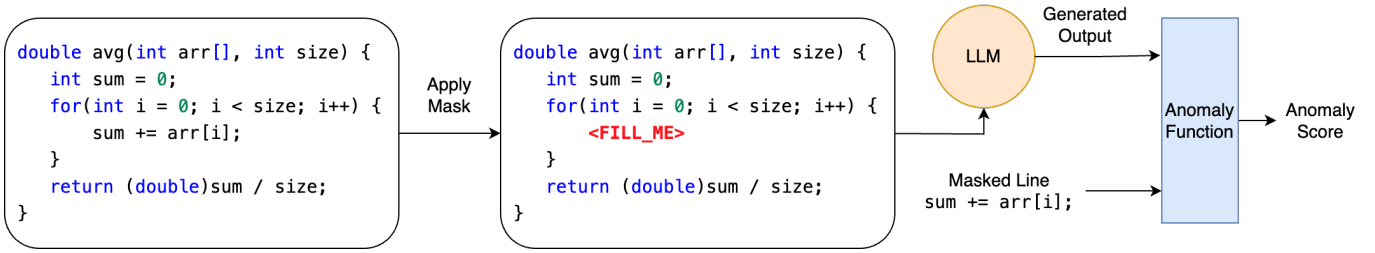


Fig. 1. Overview workflow

and reconstruction accuracy, leading to the most efficient differentiation between vulnerable and non-vulnerable lines. Additionally, when an MCS constitutes a function body, we include the function definition located above it to enrich the context.

Figure 2 illustrates an example of how we extract the compound statements associated with a masked line. We use a stack to store the line numbers of all opening braces, and then match each closing brace with the latest unmatched opening brace on the top of the stack.

C. Anomaly Score

To quantify the discrepancies between the generated line and ground truth, we assign an *anomaly score* to each line of source code. We define the anomaly score as a function which takes the masked ground truth (p) and the generated line (q) as arguments and calculates a value $\delta(p, q)$, which estimates how “anomalous” the ground truth is. A higher score suggests a greater likelihood of the current line being a vulnerability. To concretize $\delta(p, q)$, an approach used in previous studies on code naturalness [16], is to compute the cross-entropy loss for each token generated by the LLM against the masked ground truth token. By averaging the loss values across the line, we obtain an overall loss measure ($\delta_1(p, q) = \text{loss}(p, q)$). While, this loss value ranges from 0 to infinity, in practice the loss typically ranges between 0 and 1.

An alternative metric to the anomaly score is using an exact match indicator, which assigns a value of 1 if the LLM’s generated line matches the ground truth exactly, and 0 otherwise. An exact match implies that, during model inference for each token, the most probable token in each token distribution is perfectly aligned with the ground truth, and hence the line under analysis should not be considered anomalous. Thus, we can use the negation of exact string match for anomaly scoring, $\delta_2(p, q) = -\mathbb{1}_{\text{exact_match}}(p, q)$.

Using either metric alone may not fully capture the nuances of anomaly detection. The exact match indicator, being binary, produces an overly sparse distribution that may penalize slight deviations between the prediction and ground truth too harshly. The loss value, although continuous, might miss subtle yet critical discrepancies. On the one hand, it can under-estimate the level of anomaly: if a masked ground truth is “*if(a >= 0)*” and the model predicts that the line is “*if(a > 0)*”, the off-by-one-character ‘=’ might result in a low average loss but

represents a significant logical change, such as becoming the root cause of an out-of-bound array access. On the other hand, it can also over-estimate the level of anomaly: if the model has low certainty about many of the tokens in an otherwise perfectly correct prediction, it can end up computing a larger loss than the off-by-one character prediction above.

Consequently, we propose a third scoring function as outlined in Equation 1:

$$\delta(p, q) = \text{loss}(p, q) - \mathbb{1}_{\text{exact_match}}(p, q) \quad (1)$$

This hybrid approach combines both the loss and the exact match indicator, which allows us to heavily reward exact matches, signifying non-anomalous outputs; such matches typically result in a small anomaly score near -1. In comparison, non-matches, indicating anomalies, tend to result in higher scores larger than 0. However, because LLMs are prone to errors, even an exact match might still contain small possibilities that the line is vulnerable. Thus, we rely on the loss measure to capture finer discrepancies that could indicate vulnerabilities. In Section III-B, we have conducted experiments comparing all three functions, and validated that the hybrid approach offers the most reliable performance in identifying vulnerabilities as anomalous.

III. EVALUATION

This section explores the effectiveness of ANVIL’s anomaly-based vulnerability detection through five research questions. These questions investigate the different aspects of ANVIL’s design and how varying parameters affect the efficacy of vulnerability detection. Additionally, we compare ANVIL to previous vulnerability detectors and address LLM data leakage concerns.

- **RQ1:** How do different anomaly scoring methods affect the ANVIL’s vulnerability detection capability?
- **RQ2:** How does the vulnerability detection performance of ANVIL vary across different model sizes and model architectures?
- **RQ3:** Does an adaptive context size enhance vulnerability detection performance compared to a fixed context size?
- **RQ4:** How does ANVIL perform relative to supervised-learning-based vulnerability detection approaches?
- **RQ5:** Can ANVIL’s anomaly and vulnerability detection capabilities generalize to unseen data?

A. Experiment Setup

All experiments were conducted using LLMs and tokenizers from the Huggingface library [18], on a machine equipped with an Intel Xeon 4509Y CPU and an Nvidia H100 GPU with 80GB of HBM. For all LLMs, we used a temperature value of zero during code generation to prevent randomness.

We use the Magma [19] fuzzing benchmark to evaluate ANVIL’s vulnerability detection ability. The Magma benchmarks contain 138 real-world CVEs from 9 widely-used open source projects in C/C++ (libpng, libtiff, libsndfile, libxml2, poppler, openssl, sqlite3, php, lua), containing approximately 240,000 lines and 5,227 functions in total. Additionally, Magma includes both CVE (vulnerable) and patched (non-vulnerable) versions of these projects. In the vulnerable version, there are 256 lines labelled as vulnerable, of which 251 lines are located in 158 functions, while the remaining 5 lines are not associated with any function. One reason we use Magma is that as mentioned by Chen et al. [12], other popular vulnerability datasets such as BigVul [20] and CVEFixes [21] suffer from high mislabeling rates. These datasets usually consider all deleted code in a bug-fixing commit as vulnerable, potentially including irrelevant content and making the evaluation inaccurate. In contrast, the labelling of vulnerable lines in Magma is significantly more reliable because Magma developers provide a *Proof of Vulnerability* (POV) for every bug, which represents an input that triggers the vulnerability. These POVs are extracted through manual review of the bug reports and source files, as well as utilizing multiple fuzzing campaigns, ensuring all vulnerabilities in Magma are both reachable and exploitable.

Additionally, to address concerns of LLM data leakage, in RQ5, we test our methodology with vulnerabilities unseen by the LLMs. Because each LLM we tested is trained at a different time, it is difficult to find a large set of vulnerabilities that is guaranteed to be unseen by all models. Therefore, we choose to test only the CodeLlama-13B model for leakage experiments because it generally provides the best performance (as shown by having the lowest P -values in Table III). We leave the construction of leakage-free datasets and evaluation of other LLMs for future work. In total, we collected 69 CVEs from 35 different repositories using a script from the CVEFixes project [21]. All collected CVEs were published after December 31, 2023, which is later than knowledge-cutoff of the CodeLlama-13B model we used, ensuring that the CVEs are unseen by the model. Instead of only relying on lines changed by defect-fixing commits, which may contain irrelevant information, we manually inspect each commit to extract only the vulnerable lines of codes. This resulted in a dataset of 60 vulnerable source files for the leakage experiment, containing 156 vulnerable LOC with 144 located within 104 functions and 12 not associated with any specific function.

B. RQ1: Anomaly Score

To evaluate which scoring function described in Section II-C can best distinguish vulnerable lines as anomalies, we con-

ducted experiments using the CodeLlama-13B model on the Magma dataset. Specifically, we examine the distributions generated by each anomaly score for each line type (i.e. vulnerable and non-vulnerable) and evaluate the ability of each anomaly score to discriminate between the vulnerable and non-vulnerable distributions. We utilize the Mann-Whitney U test to calculate a P -value between the two distributions for each score, where a lower P -value indicates a higher statistical significance that the LLM generates different score distributions between the two line types. We have adopted the commonly utilized threshold of $\alpha = 0.05$ to determine if the two line types can be significantly distinguished, providing a confidence level of at least 95%.

We employed the FIM task, using 256 vulnerable LOC from the Magma dataset as vulnerable samples. Considering the impracticality of using over 250,000 non-vulnerable lines due to vast dataset size and time constraints, we balanced the dataset by randomly sampling 256 non-vulnerable lines for a comparative analysis. Additionally, we evaluated the vulnerability-anomaly detection capability across various fixed context sizes ranging from [500, 400, 300, 200, 100], split evenly between the prefix and the suffix surrounding the masked line. This range was selected based on observed performance metrics: context sizes smaller than 100 led to significant performance drops due to insufficient information for FIM (as illustrated in Figure 3), while sizes larger than 500 often caused out-of-memory errors on the GPU, potentially compromising evaluation accuracy.

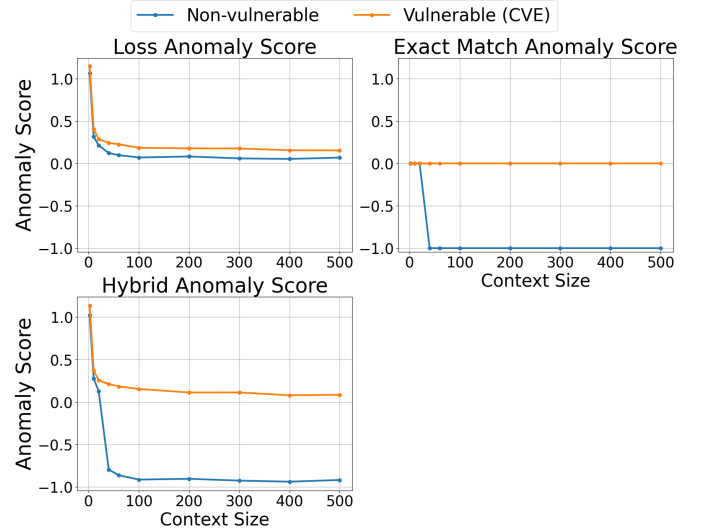


Fig. 3. Median anomaly score on various functions

For each reconstructed line of code, we calculated the anomaly scores using the aforementioned three scoring functions. Figure 3 displays three graphs, one per scoring function, with each graph showing the median anomaly scores across various fixed context sizes. We chose to plot the median value instead of the mean because, during our experiments, we observed several outliers in the anomaly scores, which could potentially skew the mean and provide a less accurate

representation of the data. We observe a noticeable performance drop when the context size is below 100 lines, but once the performance stabilizes, the results consistently show a discernible gap between vulnerable and non-vulnerable lines, reinforcing the notion that the LLM treats these two categories differently. Among the scoring functions, the gap is larger when using the hybrid function compared to only the loss function.

We then computed P -values between the distributions of scores for vulnerable and non-vulnerable lines for each scoring function and context size pair, as shown in Table I. For each context size column, we signal in bold, the scoring function that produced the lowest P -value. We can see that the combined scoring function (Equation 1) most frequently (i.e. largest number of wins) results in the smallest P -values between the two line types.

TABLE I
P-VALUES USING DIFFERENT SCORING FUNCTIONS

Function	Context Size					Wins
	100	200	300	400	500	
δ_1	7.1e-4	2.2e-4	2.7e-5	1.4e-4	0.0025	1
δ_2	4.7e-5	0.0103	6.8e-5	0.0011	0.0059	1
δ	3.3e-4	4.9e-4	9.4e-6	9.0e-5	0.0020	3

C. RQ2: Model Architecture and Model Size

While RQ1 uses CodeLlama-13B as a representative model, in this section, we investigate whether this capability of distinguishing vulnerabilities as anomalous generalizes to other LLMs. To this end, we conduct the FIM workload on various open-source code LLMs. Open-source models, unlike closed-source ones such as OpenAI’s GPT-3.5/4 series [22], provide not only the final generated tokens but also allow access to intermediate results like loss values and GPU usage, offering greater transparency and adaptability for research needs. We select the top-ranked base models from Huggingface’s Big Code Models Leaderboard as of May 1st, 2024 [23], focusing on those that support FIM code generation. To manage GPU memory efficiently, we restricted model parameters to fewer than 15 billion. Furthermore, during our evaluation, we observed that the StarCoder2-15B model exhibited poor performance on the FIM task due to an implementation bug highlighted in its original paper [24]. We thus substituted it with the StarCoderBase-15B model [25].

Additionally, we are curious about how model sizes affect the performance of distinguishing vulnerabilities as anomalous. To maintain a controlled experiment, we focused on evaluating different sizes of the same LLM architecture. Unfortunately, for CodeQwen and StarCoderBase, only one model size is available. As a result, we concentrated on CodeLlama, the only LLM with multiple model sizes suitable for the FIM task—specifically, the 7B and 13B versions.

Therefore, the evaluation involves four models, which are detailed in Table II [25]–[27]. Our experiments applied the

¹Approximated using 4 characters per token and 70 characters per LOC.

TABLE II
CODE LLMs USED IN THE EXPERIMENTS

Model Name	Model Size	Training data size ¹	Publication Time
CodeLlama	13B	29B LOC	Aug 2023
CodeLlama	7B	29B LOC	Aug 2023
CodeQwen	7B	171B LOC	Apr 2024
StarCoderBase	15B	57B LOC	May 2023

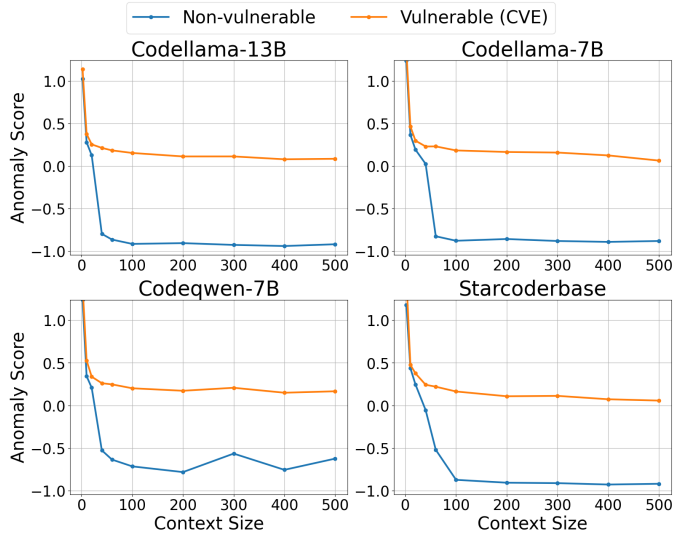


Fig. 4. Median Anomaly Score on various LLMs under different contexts

FIM task across these LLMs, assessing their median anomaly score under various fixed context sizes, as depicted in Figure 4. These figures reveal common patterns across the LLMs: 1) All models showed a drop in performance with inadequate context sizes, typically under 100 lines; 2) After LLMs acquire enough context information, their anomaly scores become stable, except for slight fluctuations observed in the CodeQwen-7B model with non-vulnerable lines; and 3) Significant gaps were observed between the scores for vulnerable and non-vulnerable lines across all models.

To precisely determine whether these LLMs can distinguish between the two line types, we calculated P -values for contexts larger than 100 lines, as shown in Table III. We can see that, all P -values consistently fell below the $\alpha = 0.05$ threshold across all models and sizes, highlighting the effectiveness of all LLMs in distinguishing vulnerable code as anomalous.

TABLE III
P-VALUES USING DIFFERENT LLMs

Function	Context Size				
	100	200	300	400	500
CodeLlama-13B	3.3e-4	4.9e-4	9.4e-6	9.0e-5	0.0020
CodeLlama-7B	0.0012	0.0019	1.2e-4	0.0026	0.0076
CodeQwen	3.9e-4	6.0e-4	3.6e-4	0.0026	0.0078
StarCoderBase	0.0010	0.0034	2.9e-4	1.4e-4	4.2e-4

When comparing different sizes of the same model, particularly CodeLlama-13B and CodeLlama-7B, the larger model

produced lower P -values for all context sizes, indicating that it has greater discriminating ability. However, this improvement is not without trade-offs. The larger CodeLlama model requires significantly more GPU memory for inference. On our H100 GPU, we discovered three samples which triggered CUDA out-of-memory errors when using large fixed context sizes; specifically, for 400 and 500 line contexts, one sample and two samples respectively trigger this error due to long line lengths. In contrast The 7B parameter model had a peak memory usage of 52GB with the same workload. This reduction in memory usage makes the smaller model a better choice when GPU memory is limited. While we have only conducted experiments on the CodeLlama models, these results are promising, and suggest that vulnerability detection accuracy should improve with neural model scaling.

D. RQ3: Adaptive Context Size

While fixed context sizes have demonstrated fairly good performance in anomaly detection, we believe that this approach can be improved for general anomaly and vulnerability discovery. A fixed context length, such as a 150-line prefix and suffix, may not sufficiently encapsulate all relevant code features for vulnerability detection. In cases where the relevant context extends beyond this 300-line window, such as in functions longer than 300 lines, critical contextual information will not be conveyed to the LLM. Conversely, in smaller functions that span only 50 lines, a 300-line context window could introduce irrelevant information. Although our previous findings suggest that this surplus information does not significantly degrade performance, it does lead to unnecessary GPU memory and computational resource usage.

As a result, we propose that utilizing the maximum compound statement (MCS) as context will improve on fixed context sizes. Using the MCS, which is typically the function body, ensures that the model receives semantically relevant context to effectively learn the code’s features without being burdened by irrelevant information that the model might inherently ignore.

After adopting MCS as our context configuration, we conducted the FIM experiment using the CodeLlama-13B model. Comparing against fixed context sizes, as shown in Figure 5, MCS significantly lowered the P -value between vulnerable and non-vulnerable lines to $1.3e-6$, a significant improvement compared to the lowest P -value obtained with a fixed 300-line context, which was $9.4e-6$. Furthermore, the MCS approach resolved the CUDA out-of-memory issues previously encountered with larger fixed contexts, reducing peak memory usage to 67GB and enhancing energy efficiency. These results illustrate an important insight—while varying fixed context size on a set of code lines has some effect on average discrimination ability, there can be specific lines where an inappropriate context size significantly confuses the model, and a dynamic context size based on code structure is better for discriminating between vulnerable and non-vulnerable code.

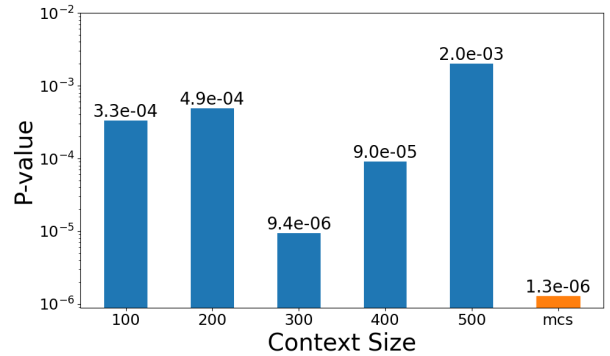


Fig. 5. P -values using fixed context sizes vs. MCS

E. RQ4: Line-level Vulnerability Detection

In this section, we compare ANVIL, which does not require any labeled vulnerability data, against two state-of-the-art supervised-learning-based vulnerability detectors: LineVul and LineVD. LineVul [8] is a software vulnerability detector that offers both function-level and line-level detection capabilities. It fine-tunes CodeBert [1] using the BigVul [20] vulnerability dataset. The detection process begins at the function level, where LineVul assesses whether a function contains any vulnerabilities. If a function is deemed vulnerable, LineVul then evaluates each line within that function. It does this by aggregating the attention scores from CodeBert’s transformer layers for each token in a line, resulting in a composite attention score for that line. A higher score means the line is more likely to be vulnerable. The intuition is that, for a vulnerability prediction task, lines with higher attention scores are deemed more critical to the model output, suggesting a greater likelihood of being linked to the root cause of the vulnerability.

LineVD [9], like LineVul, also supports both function-level and line-level detection. LineVD also uses CodeBert to generate code embeddings for each function and its constituent lines. However, it extends its analysis framework by utilizing Joern [28] to create a graph representation for each function. This graph, along with the code embeddings, are processed using a graph attention network (GAT) and a multi-layer perceptron (MLP) to simultaneously detect vulnerabilities at both the function and line levels. This system is trained on the BigVul dataset, similar to LineVul. A distinctive feature of LineVD is its *consistency mechanism*: it employs element-wise multiplication within its model to ensure that if a function is classified as non-vulnerable (label 0), then all lines within that function are also automatically classified as non-vulnerable.

In this section, all experiments are conducted using the CodeLlama-13B model with the hybrid anomaly scoring function (Equation 1) and MCS contexts. To ensure fairness and comparability in our evaluation, we will use the same metrics as those employed by our baseline models. We evaluate ANVIL vs LineVul and LineVD using two metrics: 1) We approach vulnerability detection as a binary classification task and measure the line-level classification performance using

the Area Under the Receiver Operating Characteristic Curve (ROC-AUC). This metric treats each line of code as an independent data sample, assessing the overall classification accuracy without setting a specific threshold. 2) To gauge how effective ANVIL’s anomaly score is as a vulnerability prioritization tool, we evaluate all detectors with a ranking task in which each line within a known vulnerable function is assigned a detector specific score. We then use a Top-5 metric (a standard metric for measuring vulnerability prioritization ability) to compare the detector predictions. This measure assesses whether any of the vulnerable lines are included in the detector’s top-5 most confident predictions. For this metric, each function with known vulnerabilities is treated as a separate data sample.

To enhance the reliability of our results without compromising generalizability, we utilize two mechanisms to filter out lines that are unlikely to contain vulnerabilities: M1) When a masked line is at the very beginning of the context, LLMs often misinterpret this as the start of a source file and inappropriately generate an “#include” statement. To prevent this misclassification from skewing our results, such lines are automatically considered non-vulnerable; and M2) when *both* the masked and generated outputs in the FIM task are comments, they are automatically classified as non-vulnerable. This exclusion is only applied when both are comments as cases where the model predicts that code should have been present, but a comment existed instead, may be indicative of instances where critical code is missing.

1) *Line-level Vulnerability Classification:* We first evaluate ANVIL against LineVul and LineVD regarding their capability to classify line-level vulnerabilities using ROC-AUC scores. As ANVIL operates differently from the two other tools, we have made the following adjustments.

First, although individual lines serve as the data samples for analysis, both baselines take functions instead of entire programs as inputs. As a result, we utilized the Tree-sitter [29] parsing tool to extract the 158 vulnerable functions that include the 251 vulnerable LOC, from the Magma dataset. Additionally, to mitigate potential biases from only evaluating vulnerable functions, such as characteristic differences between non-vulnerable lines in vulnerable versus non-vulnerable functions, we also selected an equal number of non-vulnerable functions (158) to match the vulnerable ones. This results in a dataset comprising 251 vulnerable LOC and 33,157 non-vulnerable LOC (totaling 33,408 LOC). This approach, while creating an imbalance, is a necessary compromise to simulate a realistic scenario in which we can understand how a detector might perform in practice.

However, LineVul depends on CodeBert for generating embeddings, which can only process up to 512 input tokens. When given a function that exceeds this limit, LineVul truncates the input to the first 512 tokens, thus only evaluating 7,075 out of the total 33,408 lines in the dataset. In contrast, ANVIL evaluates all the 33,408 lines. Additionally, given that LineVul only supports line-level detection within functions it classifies as vulnerable, for functions deemed non-vulnerable,

we automatically consider all its lines as non-vulnerable.

Furthermore, LineVD has a different method of determining which lines are considered vulnerable when comparing a CVE with its patched version. Specifically, when a patch to a vulnerability adds new lines, LineVD considers lines that are control- or data-dependent on patched lines as vulnerable lines, with the exception of the added line itself. In contrast, ANVIL would mark the line where the added line should have appeared as the location of the vulnerability. To resolve this discrepancy, we only compare vulnerabilities where the vulnerability fixing patch deletes or modifies lines, as both LineVD and ANVIL treat such lines the same way. After this adjustment, 135 LOC from 76 functions remain classified as vulnerable for this evaluation.

As shown in Table IV, after evaluating the classification performance on ANVIL and LineVul, we observed that ANVIL achieves a ROC-AUC score of 65.25%, which is 1.29 times higher than LineVul’s score of 50.66%. Similarly, compared with LineVD, ANVIL achieved a ROC-AUC score of 72.06%, while LineVD recorded a score of 70.69%. Note that ANVIL’s accuracy is different for LineVul and LineVD due to the different accommodations we had to make to the dataset for each tool. The improvement of ANVIL over LineVD is modest at 102%, yet this result is noteworthy. LineVD’s *consistency mechanism* enhances its line-level classification by leveraging insights from its function-level classifier, which can reduce false positives in non-vulnerable functions. Despite ANVIL not benefiting from similar function-level support, it still manages to achieve slightly better classification efficacy than LineVD.

TABLE IV
ANVIL VS. BASELINES

		Baseline	ANVIL
LineVul	ROC-AUC	50.66%	65.25% (129%↑)
	Top-5	26%	42.05% (162%↑)
LineVD	ROC-AUC	70.69%	72.06% (102%↑)
	Top-5	22.37%	48.68% (218%↑)

2) *Vulnerability Prioritization.:* This experiment assesses the ability of the vulnerability detectors to prioritize vulnerable lines within a given vulnerable function by comparing their Top-5 accuracies. Specifically, the Top-5 accuracy metric evaluates whether at least one vulnerable line is present among the top 5 lines ranked by these detectors. For ANVIL, lines are ranked based on the anomaly score, while LineVul uses attention scores, and LineVD employs logits from a MLP for their line ranking. In this experiment, we used the 158 vulnerable functions from Magma as our sample set.

We first compare ANVIL with LineVul. Due to the token limit issue discussed earlier, only 88 of the 158 vulnerable functions have vulnerable lines within the first 512 tokens. Thus, to ensure a fair comparison, both ANVIL and LineVul are evaluated on these 88 functions. The results, presented in Table IV, show that ANVIL significantly outperforms LineVul, with a Top-5 accuracy of 42.05% compared to LineVul’s 26%.

Comparing ANVIL with LineVD on the 76 vulnerable functions, as shown in Table IV, ANVIL achieved a Top-5 accuracy of 48.68%, markedly outperforming LineVD, which managed only 22.37%. This corresponds to an improvement of 2.18 times. Unlike the previous classification task, this evaluation on prioritization focused solely on vulnerable functions, negating the advantage of LineVD’s function-level classifier. Consequently, both tools were assessed under equivalent conditions, leading to the significantly better performance observed with ANVIL in this context.

F. RQ5: Data Leakage

In this section, we address concerns about potential data leakage that may arise if our patches for the vulnerabilities in our evaluation dataset were present in the LLM training data, as this may enable the LLM to correctly generate the patched code instead of the vulnerable code, as discussed in Section I and III-A. Due to time constraints and the extensive scope of validations required across multiple models, this evaluation is primarily conducted on the CodeLlama-13B model. For this experiment, we continue to use the hybrid scoring function and MCS configuration.

We begin by assessing ANVIL’s ability to detect vulnerable lines as anomalies within the 2024 CVEFixes dataset, which includes 156 vulnerable lines. To ensure a balanced evaluation, we also randomly selected an equal number of 156 non-vulnerable lines from the same source files. The result indicates a P -value of $5.4e-6$ between vulnerable and non-vulnerable lines, which is significantly lower than the $\alpha = 0.05$ threshold and is comparable to the P -value obtained in the Magma dataset ($1.3e-6$, from Figure 5). These findings confirm that ANVIL’s vulnerability-anomaly detection capabilities are not tied to dataset exposure and can generalize to unseen vulnerabilities.

Furthermore, to assess the generalizability of ANVIL in detecting line-level vulnerabilities, we evaluated its performance on both our leakage-free 2024 CVEFixes dataset and the *entire* Magma dataset. Note that earlier experiments with Magma only utilize a subset to accommodate comparison with previous detectors. Similar to previous experiments (section III-E), we evaluate vulnerability classification through ROC-AUC scores. For the CVEFixes dataset, we analyzed a total of 208 functions—comprising an equal split of 104 vulnerable and 104 non-vulnerable functions—from the 2024 CVEFixes dataset. This dataset encompasses 12,402 LOC. The results, shown in Table V, demonstrate that ANVIL maintains consistent ROC-AUC scores across both datasets, achieving 67.20% on the CVEFixes dataset, compared with 65.25% on the Magma dataset. This consistency demonstrates the robustness of ANVIL’s vulnerability detection capabilities across diverse datasets.

For the evaluation of vulnerability prioritization, we focused on the 104 vulnerable functions containing 144 vulnerable lines from the 2024 CVEFixes dataset. To provide a comparative analysis with the Magma dataset, we re-executed the prioritization experiment using all 158 vulnerable functions it

contains. Results in Table V reveal that the Top-5 accuracy on the CVEFixes dataset is slightly lower than that observed with Magma. This discrepancy can be attributed to the manual inspection process used for the CVEFixes dataset, detailed in Section III-A, where our limited familiarity with the code bases might have led to some vulnerabilities being overlooked and incorrectly labelled as non-vulnerable. These overlooked vulnerabilities might appear among the top 5 predictions from ANVIL, contributing to the nominally lower Top-5 accuracy. To mitigate the effects of this potential mislabeling, we extended our analysis to include Top-10 accuracy, providing a more lenient criterion that better captures ANVIL’s performance. In this broader evaluation, ANVIL achieved a Top-10 accuracy of 51.92% on the CVEFixes dataset, slightly outperforming the 48.73% observed with Magma, confirming that our anomaly-based approach is robust and not compromised by data leakage in its ability to prioritize vulnerabilities accurately.

TABLE V
ANVIL’S GENERALIZABILITY OF VULNERABILITY DETECTION

	ROC-AUC	Top-5	Top-10
Magma	65.25%	34.18%	48.73%
2024 CVEFixes	67.20%	23.08%	51.92%

IV. DISCUSSION

A. Mechanisms in Line-level Vulnerability Detection

In Section III-E, we evaluated ANVIL for line-level vulnerability detection using the anomaly score (AS) as the foundation, supplemented by two additional filtering mechanisms, M1 and M2, designed to exclude lines unlikely to contain vulnerabilities. To assess the individual contributions of these mechanisms, we conducted an ablation study.

Table VI presents the impact of each component. For clarity and context, we include the baseline performance of ANVIL without any mechanisms and with an anomaly score of 0 for all lines, akin to random guessing, at the bottom of the table. The inclusion of anomaly score alone yielded improvements of 1.12 times in ROC-AUC and 1.1 times in Top-5 accuracy over random guessing. Adding M1 further enhanced the ROC-AUC to 57%, though it did not impact the Top-5 accuracy. However, for Top-10 accuracy, M1’s inclusion increased the accuracy marginally from 43% to 43.7%. When employing all three mechanisms together, there was a substantial increase in both ROC-AUC and Top-5 accuracy, achieving 31% and 32% improvements respectively compared to the baseline.

TABLE VI
ABLATION STUDY

AS	M1	M2	ROC-AUC	Top-5	Top-10
✓	✓	✓	65.3% (+31%↑)	34.2% (+32%↑)	48.7% (+48%↑)
✓	✓		57.0% (+14%↑)	28.5% (+10%↑)	43.7% (+33%↑)
✓			56.1% (+12%↑)	28.5% (+10%↑)	43.0% (+31%↑)
Random			50%	26.0%	32.9%

B. Vulnerable vs Patched lines

In addition to collecting vulnerable and non-vulnerable lines, we also gathered 353 patched lines from the Magma dataset for the 138 known CVEs. These lines include the additions and modifications made to address the CVEs. Additionally, when a defect-fixing commit deletes a line, we also include the subsequent line in the same location as part of the patched lines.

While our primary focus remains on vulnerability detection, an intriguing pattern emerged regarding these patched lines. To elucidate, we examined the exact match accuracy (the proportion of lines where the generated output exactly matches the ground truth) across all line types under various contexts, depicted on the left side of Figure 6. Expectedly, non-vulnerable lines exhibited higher exact match accuracies compared to vulnerable lines, but notably, patched lines consistently showed intermediate accuracy levels.

Further analysis using the median anomaly scores under fixed context sizes revealed that patched lines generally align closely with non-vulnerable lines, albeit slightly higher. This trend shifts markedly under the maximum compound statement (MCS) context, where the exact match accuracy for patched lines drops below 50%, causing their median anomaly scores to approach those of vulnerable lines (see Figure 6 right).

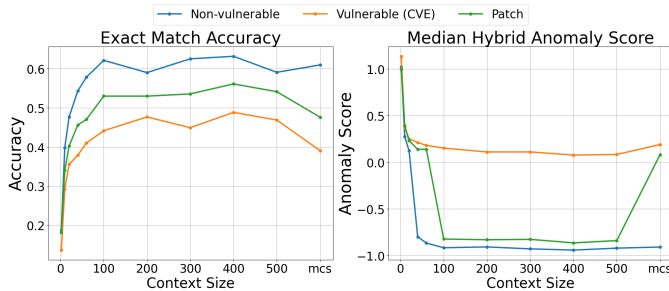


Fig. 6. Patch vs. CVE vs. Non-vulnerable Lines

To probe deeper, we assessed the statistical significance between patched and other line types using P-values (Table VII). All P-values comparing patched to vulnerable lines fell below the $\alpha = 0.05$ threshold, suggesting significant differences. Conversely, the P-values comparing patched to non-vulnerable lines were above this threshold but still displayed relatively low confidence levels (four of six numbers range from 8.36% to 26.67%).

TABLE VII
PATCH VS. CVE VS. NON-VULNERABLE LINES IN P-VALUES

P-value	Context Size					
	100	200	300	400	500	mcs
Patch vs. Vul	0.0040	0.0048	0.0037	0.0035	0.0209	0.0047
Patch vs. Non-vul	0.7944	0.2667	0.1266	0.5102	0.2647	0.0836

The conclusion we draw from these experiments is that even after a vulnerability has been patched, the code that fixes the

vulnerability still exhibits some statistical differences with regular code. One potential explanation is that some percentage of patched code is still vulnerable which is consistent with insights from the Magma study [19], so the patched lines are actually a mix of vulnerable and non-vulnerable code. Another potential explanation is that the code locations where vulnerabilities tend to exist may simply have higher entropy, or depend on global factors, which makes it difficult for current LLMs (and possibly their human counterparts) to generate correctly.

V. THREATS TO VALIDITY

Internal Validity. One threat to internal validity lies in data labelling. Correctly labelling which lines are vulnerable continues to be a challenging problem, as vulnerabilities are often difficult to isolate and determining what code is considered vulnerable can take a wide array of definitions. To mitigate this, we use the Magma dataset for our vulnerability detection experiments (RQ1-4). As mentioned in section III, all labelled vulnerabilities in Magma are provided with a POV through extensive manual review and fuzzing campaigns, which ensures that lines labelled as vulnerable are indeed related to the vulnerabilities. Further, manual labelling by a small set of developers, results in better consistency that is less impacted by different definitions of "vulnerable" that may arise in datasets scraped from CVE reports. For the leakage experiment (RQ5), we manually curate the 2024 CVE-Fixes datasets to ensure the correctness of the labelling. However, while manual curation on its own is likely to have fewer mislabels than simply scraping data from CVE reports, it can still be imperfect due to the complex structure and the large code base of the included projects.

External Validity. While we demonstrated in Section III-F that ANVIL generalizes to non-leakage data by evaluating its consistency across the Magma and 2024 CVEFixes datasets, we concede that numerically comparing the accuracy across two data sets may yield an imprecise conclusion since the two datasets are composed of two different samples of vulnerabilities, and it is nearly impossible to control for this. While we could increase the number of samples in both datasets to decrease chances of sample error, manually finding and reproducing real vulnerabilities is manually intensive and difficult. Future research could aim to collect a more extensive non-leakage dataset to conduct a larger-scale evaluation, providing a more robust statistical comparison of ANVIL's generalizability to non-leakage data.

Construct Validity. To comment on our selection of measurements, we use common metrics that are also employed in other works to evaluate the vulnerability detection capability of all examined tools. Additionally, we set the temperature of the LLMs used in our experiments to 0 to remove any potential randomness in the generation of output.

VI. RELATED WORK

Anomaly Detection. Previous work has used anomalous behaviour as a signal for buggy code. Yun et al. [30] detects API

misuse by automatically modelling correct usage patterns from existing code. They use this model to detect anomalous uses, and hence bugs. Other work from Ahmadi et al. [31] operates on singular codebases and clusters functionally similar yet inconsistent code. Their insight is that small inconsistencies between code that should have the same functionality can lead to bugs (e.g. missing checks). To our knowledge, the only previous attempt to leverage LLMs for anomaly-guided vulnerability detection used a simple string distance score between the LLM prediction and ground truth to determine if a line of source code is anomalous [32]. A string distance calculation lacks any contextual understanding of the strings being compared, and ANVIL improves upon this with a cross-entropy based anomaly measure. Further, their method of detecting anomalies relies heavily on pre-existing source code comments; our approach makes no assumptions on the contents of the software under examination. Finally, LLM-based anomaly detection in other non-code domains has also been explored, especially in log analysis and network intrusion detection [33].

LLMs. Following the success of natural language generation with LLMs, work such as CodeBERT [1] and CodeT5 [2] have applied transformers toward code generation and understanding. CodeBERT is an encoder-only transformer that supports bidirectional natural language-programming language generation. However, it requires an additional decoder layer that cannot benefit from pre-training. To address this, Wang et al. proposed CodeT5, an encoder-decoder transformer. CodeT5 is pre-trained on tasks in which source code identifiers, and entire spans of code are masked for prediction. VulGen [13], extends previous work by training an LLM to identify and inject vulnerabilities into the codebase of programs for the purposes of synthetic data generation.

ML-Assisted Dynamic Vulnerability Detection. Many existing fuzzers have leveraged machine learning to boost fuzzer performance. He et al. [34] demonstrated a neural network’s ability to imitate the behaviour of a symbolic execution engine. They use a symbolic engine to generate input transactions to a corpus of smart contracts. They then train a neural network to predict these transactions. The network is then integrated into a fuzzer which they use to test unseen smart contracts. Recent work from Shi et al. [35] uses a convolutional neural network to classify the behaviour of basic blocks. They then correlate these basic blocks with bytes in the program input. They use this mapping from input bytes to classification to guide an input-format-aware fuzzer. As for LLMs, a recent paper utilized ChatGPT to parse protocol specifications into a machine understandable grammar, which they then integrate into a protocol aware fuzzer [36].

ML-Assisted Static Vulnerability Detection. To detect use-before-initialization bugs, Li et al. [37] augments a state-of-the-art static analysis tool with an LLM prompting technique. They utilize the LLM to extract variable initialization information when the static analysis tool is unable to handle certain code features (i.e. unsupported library calls). Conversely, Sun et al. [38] first utilizes an LLM to match

candidate source code with potential vulnerabilities, then uses static analysis to verify its legitimacy. They apply their method to find vulnerabilities in smart contracts.

ML-Based Vulnerability Detection. ML-based vulnerability detection largely focuses on the architecture and code features that will better lead a model to automatically detect vulnerabilities. An early approach from Russell et al. [11] attempts to find C/C++ vulnerabilities with a convolutional neural network. Further advances have experimented with graph neural networks [5] and long short-term memory models [4]. Unfortunately, on unseen bugs, these architecture level differences have not resulted in generalization to unseen, real-world vulnerabilities [39], and other work shows the same trend for prompt-guided LLM-based detectors [3]. Other work has focused on using different code features for training vulnerability detectors, such as code slices [10] and bug-triggering paths [7].

VII. CONCLUSION

To address the limitations of existing supervised-learning-based vulnerability detectors, we propose ANVIL, which leverages model mispredictions as guidance for software vulnerability detection. Our method capitalizes on the inherent capabilities of LLMs to generate normatively correct code, utilizing discrepancies in the model’s predictions to flag potential vulnerabilities. By employing code generation tasks across different LLMs, we have shown that this discrepancy in vulnerabilities is generalized to different model sizes and model architectures, and we also reveal that using compound statement contexts (MCS) outperforms simpler fix-sized contexts, providing a more relevant and precise framework for evaluating vulnerabilities. Furthermore, comparative evaluations against state-of-the-art supervised models LineVul and LineVD highlight ANVIL’s superior performance, achieving significantly better ROC-AUC and Top-5 accuracy metrics without the need for a labelled training dataset.

REFERENCES

- [1] Z. Feng, D. Guo, D. Tang, N. Duan, X. Feng, M. Gong, L. Shou, B. Qin, T. Liu, D. Jiang, and M. Zhou, “CodeBERT: A Pre-Trained Model for Programming and Natural Languages,” Sep. 2020, arXiv:2002.08155 [cs]. [Online]. Available: <http://arxiv.org/abs/2002.08155>
- [2] Y. Wang, W. Wang, S. Joty, and S. C. H. Hoi, “CodeT5: Identifier-aware Unified Pre-trained Encoder-Decoder Models for Code Understanding and Generation,” Sep. 2021, arXiv:2109.00859 [cs]. [Online]. Available: <http://arxiv.org/abs/2109.00859>
- [3] B. Steenhoeck, M. M. Rahman, M. K. Roy, M. S. Alam, E. T. Barr, and W. Le, “A Comprehensive Study of the Capabilities of Large Language Models for Vulnerability Detection,” Mar. 2024, arXiv:2403.17218 [cs]. [Online]. Available: <http://arxiv.org/abs/2403.17218>
- [4] Z. Li, D. Zou, S. Xu, X. Ou, H. Jin, S. Wang, Z. Deng, and Y. Zhong, “VulDeePecker: A Deep Learning-Based System for Vulnerability Detection,” in *Proceedings 2018 Network and Distributed System Security Symposium*, 2018, arXiv:1801.01681 [cs]. [Online]. Available: <http://arxiv.org/abs/1801.01681>
- [5] X. Cheng, H. Wang, J. Hua, G. Xu, and Y. Sui, “DeepWukong: Statically Detecting Software Vulnerabilities Using Deep Graph Neural Network,” *ACM Transactions on Software Engineering and Methodology*, vol. 30, no. 3, pp. 1–33, May 2021. [Online]. Available: <https://dl.acm.org/doi/10.1145/3436877>

- [6] Y. Li, S. Wang, and T. N. Nguyen, "Vulnerability detection with fine-grained interpretations," in *Proceedings of the 29th ACM Joint Meeting on European Software Engineering Conference and Symposium on the Foundations of Software Engineering*, ser. ESEC/FSE 2021. New York, NY, USA: Association for Computing Machinery, Aug. 2021, pp. 292–303. [Online]. Available: <https://doi.org/10.1145/3468264.3468597>
- [7] X. Cheng, X. Nie, N. Li, H. Wang, Z. Zheng, and Y. Sui, "How About Bug-Triggering Paths? - Understanding and Characterizing Learning-Based Vulnerability Detectors," *IEEE Transactions on Dependable and Secure Computing*, pp. 1–18, 2022. [Online]. Available: <https://ieeexplore.ieee.org/document/9833339/>
- [8] M. Fu and C. Tantithamthavorn, "LineVul: a transformer-based line-level vulnerability prediction," in *Proceedings of the 19th International Conference on Mining Software Repositories*. Pittsburgh Pennsylvania: ACM, May 2022, pp. 608–620. [Online]. Available: <https://dl.acm.org/doi/10.1145/3524842.3528452>
- [9] D. Hin, A. Kan, H. Chen, and M. A. Babar, "LineVD: statement-level vulnerability detection using graph neural networks," in *Proceedings of the 19th International Conference on Mining Software Repositories*. Pittsburgh Pennsylvania: ACM, May 2022, pp. 596–607. [Online]. Available: <https://dl.acm.org/doi/10.1145/3524842.3527949>
- [10] Y. Mirsky, G. Macon, M. Brown, C. Yagemann, M. Pruett, E. Downing, S. Mertoguno, and W. Lee, "{VulChecker}: Graph-based Vulnerability Localization in Source Code," 2023, pp. 6557–6574. [Online]. Available: <https://www.usenix.org/conference/usenixsecurity23/presentation/mirsky>
- [11] R. Russell, L. Kim, L. Hamilton, T. Lazovich, J. Harer, O. Ozdemir, P. Ellingwood, and M. McConley, "Automated Vulnerability Detection in Source Code Using Deep Representation Learning," in *2018 17th IEEE International Conference on Machine Learning and Applications (ICMLA)*, Dec. 2018, pp. 757–762. [Online]. Available: <https://ieeexplore.ieee.org/abstract/document/8614145>
- [12] Y. Chen, Z. Ding, L. Alowain, X. Chen, and D. Wagner, "DiverseVul: A New Vulnerable Source Code Dataset for Deep Learning Based Vulnerability Detection," in *Proceedings of the 26th International Symposium on Research in Attacks, Intrusions and Defenses*, ser. RAID '23. New York, NY, USA: Association for Computing Machinery, Oct. 2023, pp. 654–668. [Online]. Available: <https://doi.org/10.1145/3607199.3607242>
- [13] Y. Nong, Y. Ou, M. Pradel, F. Chen, and H. Cai, "VULGEN: Realistic Vulnerability Generation Via Pattern Mining and Deep Learning," in *2023 IEEE/ACM 45th International Conference on Software Engineering (ICSE)*. Melbourne, Australia: IEEE, May 2023, pp. 2527–2539. [Online]. Available: <https://ieeexplore.ieee.org/document/10172870/>
- [14] Y. Nong, R. Fang, G. Yi, K. Zhao, X. Luo, F. Chen, and H. Cai, "VGX: Large-Scale Sample Generation for Boosting Learning-Based Software Vulnerability Analyses," in *Proceedings of the IEEE/ACM 46th International Conference on Software Engineering*. Lisbon Portugal: ACM, Apr. 2024, pp. 1–13. [Online]. Available: <https://dl.acm.org/doi/10.1145/3597503.3639116>
- [15] A. Hindle, E. T. Barr, M. Gabel, Z. Su, and P. Devanbu, "On the naturalness of software," *Communications of the ACM*, vol. 59, no. 5, pp. 122–131, Apr. 2016. [Online]. Available: <https://dl.acm.org/doi/10.1145/2902362>
- [16] B. Ray, V. Hellendoorn, S. Godhane, Z. Tu, A. Bacchelli, and P. Devanbu, "On the "naturalness" of buggy code," in *Proceedings of the 38th International Conference on Software Engineering*, ser. ICSE '16. New York, NY, USA: Association for Computing Machinery, May 2016, pp. 428–439. [Online]. Available: <https://dl.acm.org/doi/10.1145/2884781.2884848>
- [17] M. Bavarian, H. Jun, N. Tezak, J. Schulman, C. McLeavey, J. Tworek, and M. Chen, "Efficient Training of Language Models to Fill in the Middle," Jul. 2022, arXiv:2207.14255 [cs]. [Online]. Available: <http://arxiv.org/abs/2207.14255>
- [18] T. Wolf, L. Debut, V. Sanh, J. Chaumond, C. Delangue, A. Moi, P. Cistac, T. Rault, R. Louf, M. Funtowicz, J. Davison, S. Shleifer, P. von Platen, C. Ma, Y. Jernite, J. Plu, C. Xu, T. Le Scao, S. Gugger, M. Drame, Q. Lhoest, and A. Rush, "Transformers: State-of-the-Art Natural Language Processing," in *Proceedings of the 2020 Conference on Empirical Methods in Natural Language Processing: System Demonstrations*, Q. Liu and D. Schlangen, Eds. Online: Association for Computational Linguistics, Oct. 2020, pp. 38–45. [Online]. Available: <https://aclanthology.org/2020.emnlp-demos.6>
- [19] A. Hazimeh, A. Herrera, and M. Payer, "Magma: A Ground-Truth Fuzzing Benchmark," *Proceedings of the ACM on Measurement and Analysis of Computing Systems*, vol. 4, no. 3, pp. 49:1–49:29, Nov. 2020. [Online]. Available: <https://dl.acm.org/doi/10.1145/3428334>
- [20] J. Fan, Y. Li, S. Wang, and T. N. Nguyen, "A C/C++ Code Vulnerability Dataset with Code Changes and CVE Summaries," in *Proceedings of the 17th International Conference on Mining Software Repositories*, ser. MSR '20. New York, NY, USA: Association for Computing Machinery, 2020, pp. 508–512. [Online]. Available: <https://doi.org/10.1145/3379597.3387501>
- [21] G. Bhandari, A. Naseer, and L. Moonen, "CVEfixes: automated collection of vulnerabilities and their fixes from open-source software," in *Proceedings of the 17th International Conference on Predictive Models and Data Analytics in Software Engineering*, ser. PROMISE 2021. New York, NY, USA: Association for Computing Machinery, 2021, pp. 30–39. [Online]. Available: <https://doi.org/10.1145/3475960.3475985>
- [22] "ChatGPT." [Online]. Available: <https://openai.com/chatgpt/>
- [23] "Big Code Models Leaderboard - a Hugging Face Space by bigcode." [Online]. Available: <https://huggingface.co/spaces/bigcode/bigcode-models-leaderboard>
- [24] A. Lozhkov, R. Li, L. B. Allal, F. Cassano, J. Lamy-Poirier, N. Tazi, A. Tang, D. Pykhtar, J. Liu, Y. Wei, T. Liu, M. Tian, D. Kocetkov, A. Zucker, Y. Belkada, Z. Wang, Q. Liu, D. Abulkhanov, I. Paul, Z. Li, W.-D. Li, M. Risdal, J. Li, J. Zhu, T. Y. Zhuo, E. Zheltonozhskii, N. O. O. Dade, W. Yu, L. Krauß, N. Jain, Y. Su, X. He, M. Dey, E. Abati, Y. Chai, N. Muennighoff, X. Tang, M. Oblokulov, C. Akiki, M. Marone, C. Mou, M. Mishra, A. Gu, B. Hui, T. Dao, A. Zebaze, O. Dehaene, N. Patry, C. Xu, J. McAuley, H. Hu, T. Scholak, S. Paquet, J. Robinson, C. J. Anderson, N. Chapados, M. Patwary, N. Tajbakhsh, Y. Jernite, C. M. Ferrandis, L. Zhang, S. Hughes, T. Wolf, A. Guha, L. von Werra, and H. de Vries, "StarCoder 2 and The Stack v2: The Next Generation," Feb. 2024, arXiv:2402.19173 [cs]. [Online]. Available: <http://arxiv.org/abs/2402.19173>
- [25] R. Li, L. B. Allal, Y. Zi, N. Muennighoff, D. Kocetkov, C. Mou, M. Marone, C. Akiki, J. Li, J. Chim, Q. Liu, E. Zheltonozhskii, T. Y. Zhuo, T. Wang, O. Dehaene, M. Davaadorj, J. Lamy-Poirier, J. Monteiro, O. Shliazhko, N. Gontier, N. Meade, A. Zebaze, M.-H. Yee, L. K. Umaphathi, J. Zhu, B. Lipkin, M. Oblokulov, Z. Wang, R. Murthy, J. Stillerman, S. S. Patel, D. Abulkhanov, M. Zocca, M. Dey, Z. Zhang, N. Fahmy, U. Bhattacharyya, W. Yu, S. Singh, S. Luccioni, P. Villegas, M. Kunakov, F. Zhdanov, M. Romero, T. Lee, N. Timor, J. Ding, C. Schlesinger, H. Schoelkopf, J. Ebert, T. Dao, M. Mishra, A. Gu, J. Robinson, C. J. Anderson, B. Dolan-Gavitt, D. Contractor, S. Reddy, D. Fried, D. Bahdanau, Y. Jernite, C. M. Ferrandis, S. Hughes, T. Wolf, A. Guha, L. von Werra, and H. de Vries, "StarCoder: may the source be with you!" Dec. 2023, arXiv:2305.06161 [cs]. [Online]. Available: <http://arxiv.org/abs/2305.06161>
- [26] B. Rozière, J. Gehring, F. Gloeckle, S. Sootla, I. Gat, X. E. Tan, Y. Adi, J. Liu, R. Sauvestre, T. Remez, J. Rapin, A. Kozhevnikov, I. Evtimov, J. Bitton, M. Bhatt, C. C. Ferrer, A. Grattafiori, W. Xiong, A. Défossez, J. Copet, F. Azhar, H. Touvron, L. Martin, N. Usunier, T. Scialom, and G. Synnaeve, "Code Llama: Open Foundation Models for Code," Jan. 2024, arXiv:2308.12950 [cs]. [Online]. Available: <http://arxiv.org/abs/2308.12950>
- [27] Q. Team, "Code with CodeQwen1.5," Apr. 2024, section: blog. [Online]. Available: <http://qwenlm.github.io/blog/codeqwen1.5/>
- [28] "Joern - The Bug Hunter's Workbench." [Online]. Available: <https://joern.io/>
- [29] "tree-sitter/tree-sitter," Jul. 2024. [Online]. Available: <https://github.com/tree-sitter/tree-sitter>
- [30] I. Yun, C. Min, X. Si, Y. Jang, T. Kim, and M. Naik, "{APISan}: Sanitizing {API} Usages through Semantic {Cross-Checking}," 2016, pp. 363–378. [Online]. Available: <https://www.usenix.org/conference/usenixsecurity16/technical-sessions/presentation/yun>
- [31] M. Ahmadi, R. M. Farkhani, R. Williams, and L. Lu, "Finding Bugs Using Your Own Code: Detecting Functionally-similar yet Inconsistent Code," 2021, pp. 2025–2040. [Online]. Available: <https://www.usenix.org/conference/usenixsecurity21/presentation/ahmadi>
- [32] B. Ahmad, B. Tan, R. Karri, and H. Pearce, "FLAG: Finding Line Anomalies (in code) with Generative AI," Jun. 2023, arXiv:2306.12643 [cs]. [Online]. Available: <http://arxiv.org/abs/2306.12643>
- [33] J. Su, C. Jiang, X. Jin, Y. Qiao, T. Xiao, H. Ma, R. Wei, Z. Jing, J. Xu, and J. Lin, "Large Language Models for Forecasting and

- Anomaly Detection: A Systematic Literature Review,” Feb. 2024, arXiv:2402.10350 [cs]. [Online]. Available: <http://arxiv.org/abs/2402.10350>
- [34] J. He, M. Balunović, N. Ambroladze, P. Tsankov, and M. Vechev, “Learning to Fuzz from Symbolic Execution with Application to Smart Contracts,” in *Proceedings of the 2019 ACM SIGSAC Conference on Computer and Communications Security*, ser. CCS ’19. New York, NY, USA: Association for Computing Machinery, 2019, pp. 531–548. [Online]. Available: <https://doi.org/10.1145/3319535.3363230>
- [35] J. Shi, Z. Wang, Z. Feng, Y. Lan, S. Qin, W. You, W. Zou, M. Payer, and C. Zhang, “AIFORE: Smart fuzzing based on automatic input format reverse engineering,” in *32nd USENIX Security Symposium (USENIX Security 23)*. Anaheim, CA: USENIX Association, Aug. 2023, pp. 4967–4984. [Online]. Available: <https://www.usenix.org/conference/usenixsecurity23/presentation/shi-ji>
- [36] R. Meng, M. Mirchev, M. Böhme, and A. Roychoudhury, “Large Language Model guided Protocol Fuzzing,” in *Proceedings 2024 Network and Distributed System Security Symposium*. San Diego, CA, USA: Internet Society, 2024. [Online]. Available: <https://www.ndss-symposium.org/wp-content/uploads/2024-556-paper.pdf>
- [37] H. Li, Y. Hao, Y. Zhai, and Z. Qian, “Enhancing Static Analysis for Practical Bug Detection: An LLM-Integrated Approach,” vol. 8, 2024.
- [38] Y. Sun, D. Wu, Y. Xue, H. Liu, H. Wang, Z. Xu, X. Xie, and Y. Liu, “GPTScan: Detecting Logic Vulnerabilities in Smart Contracts by Combining GPT with Program Analysis,” in *Proceedings of the IEEE/ACM 46th International Conference on Software Engineering*, ser. ICSE ’24. New York, NY, USA: Association for Computing Machinery, Apr. 2024, pp. 1–13. [Online]. Available: <https://dl.acm.org/doi/10.1145/3597503.3639117>
- [39] S. Chakraborty, R. Krishna, Y. Ding, and B. Ray, “Deep Learning Based Vulnerability Detection: Are We There Yet?” *IEEE Transactions on Software Engineering*, vol. 48, no. 9, pp. 3280–3296, Sep. 2022, conference Name: IEEE Transactions on Software Engineering. [Online]. Available: <https://ieeexplore.ieee.org/abstract/document/9448435>